



## Original Research Article

## Green synthesis of nanocellulose fibers from ragi stalk and its characterization

Prasanna Kumar Jammapura Kallappa<sup>a,\*</sup>, Prakash Gowdra Kalleshappa<sup>b</sup>, Suresh Basavarajappa<sup>c</sup>, Basavarajappa Bachi Eshwarappa<sup>a</sup>

<sup>a</sup> Research Centre, Department of Chemistry, Bapuji Institute of Engineering and Technology (Affiliated to Visvesvaraya Technological University, Belagavi) Davangere, Karnataka 577004, India

<sup>b</sup> Department of Chemistry, STJPU College, Davangere, Karnataka 577004, India

<sup>c</sup> Department of Civil Engineering, Bapuji Institute of Engineering and Technology (Affiliated to Visvesvaraya Technological University, Belagavi), Davangere, Karnataka 577004, India

## ARTICLE INFORMATION

Received: 10 August 2022

Received in revised: 19 September 2022

Accepted: 20 September 2022

Available online: 6 October 2022

DOI: 10.22034/ajgc.2022.3.7

## KEYWORDS

Ragi Stalk

Green Solvent

Ionic liquid

Cellulose

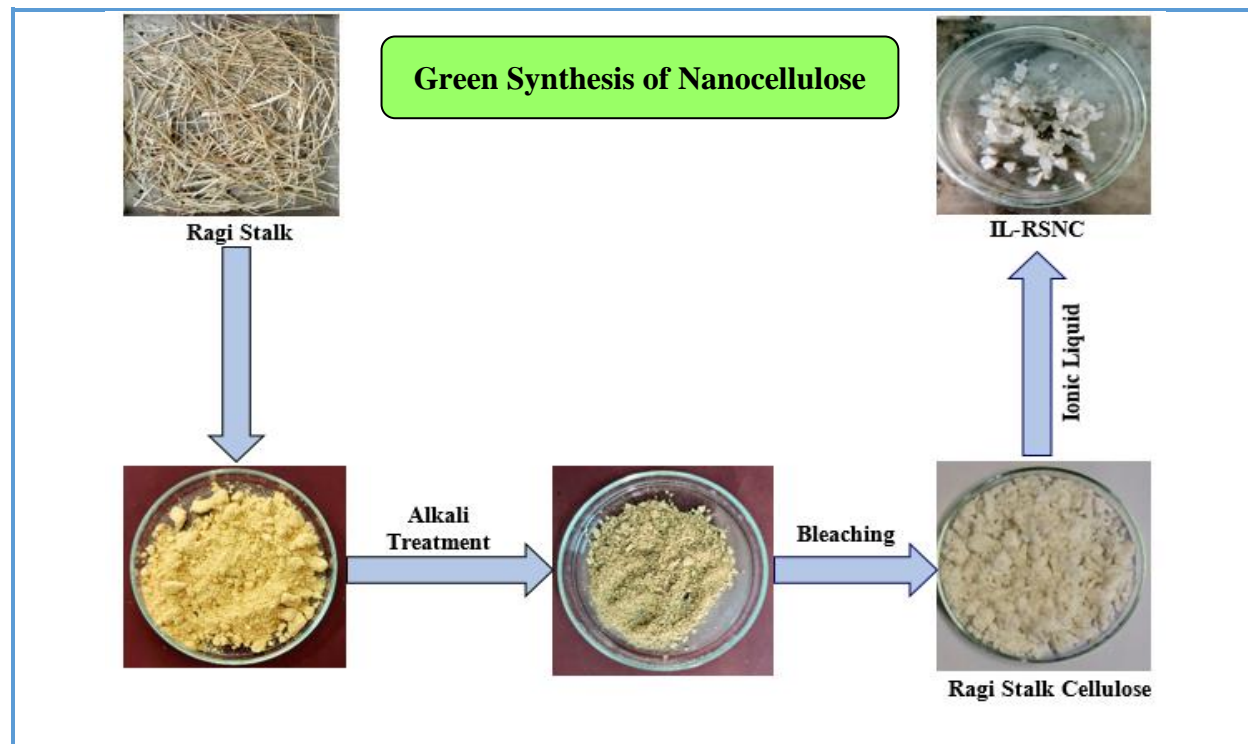
Nanocellulose

## ABSTRACT

Nanocellulose derived from natural substances offers a plethora of opportunities to produce superior material properties for various applications. In the present study, nanocellulose was extracted from Ragi Stalk (*Eleusine Coracana*) an abundantly available agricultural biomass. The cellulose was alkali-treated followed by bleaching to remove hemicellulose, Pectins, wax, and lignin. Green solvent i.e. ionic liquid (1-butyl-3-methylimidazolium chloride ([Bmim]Cl)) was used to synthesize the nanocellulose through sonication and centrifugation. The FT-IR spectra reveal the functional groups and substantial conversion of cellulose to nanocellulose. The crystallinity of synthesized nanocellulose is illustrated by XRD. The surface architecture and the obtained nanocellulose size are represented by SEM and TEM monographs. The new finding is that the TEM images show the synthesized nanocellulose fibres have a smaller dimension between 14.58 and 22.17 nm evidenced through sonication. The thermal stability of the obtained nanocellulose was evidenced by using TGA/DTA. The thermal studies record that synthesized nanocellulose fibres shows phenomenal thermal stability up to 460 °C.

© 2022 by SPC (Sami Publishing Company), Asian Journal of Green Chemistry, Reproduction is permitted for noncommercial purposes.

## Graphical Abstract



## Introduction

The energy sectors around the world are facing challenges to meet the demand and supply gap of energy as a result of population growth and industrial globalization. After coal and oil, biomass, and a carbon-neutral renewable resource derived from the carbon-containing waste of diverse natural and anthropogenic processes has emerged as the third primary energy resource to close the energy gap. Biomass could be generated from different sources, including the timber industry besides, agriculture sector crops, forest raw materials, significant parts of domestic wastes, and wood. As a result, researchers and developers are increasing their focus aside from coal and oil and toward biomass, which will produce carbon-neutral energy and solve a range of problems such as the management of

solid waste, health implications, and bushfires [1].

As a developing nation, India has battled for decades to comply with the global environmental and solid-waste management norms, which has been a significant obstacle. It generates an annual average of 960-1000 million tonnes of solid waste, with the agricultural sector accounting for a large portion of this [2]. Post-harvesting is responsible for about 13% of all solid waste made in Asia [3]. India is one of the top three countries that grow maize, paddy, and wheat, so researchers are most interested in how to use the type of cellulose that comes from these crops. The most under-utilized forms of cellulose, according to the current research scenario, are Ragi Stalk, mango wood, rice husk, sugar cane, and peanut shell [4, 5]. With 50% of the workforce employed in agriculture. India is self-sufficient in natural cellulose, and there is

an abundance of bio-waste. Countries such as the United States, Europe, Canada, and Australia prioritize nanocellulose production due to its practical application in commercial products [6-8]. In terms of nature, size, and function, nanocellulose is largely dependent on its parent cellulose.

The recent years have seen the nanotechnology growth, which is interconnected with numerous other scientific disciplines and has an impact on all kinds of life [9]. Nanotechnology is a discipline of science that focuses on the development, modification, and application of materials with nanometer-scale dimensions. Nanotechnology is essential to the study of nanoparticles due to their diverse uses [10]. Cellulose and lignocellulose nanoparticles play a vital role in nanotechnology. The cellulosic materials are the most prevalent biological raw materials and can self-assemble into well-defined designs of numerous sizes, from nano to micro. Moreover, cellulose is a multipurpose raw material that can replace a number of non-renewable substances [11].

Cellulose nanocrystals (CNCs) and cellulose nanofibrils are the two major types of cellulose nanomaterials (CNs) that can be derived from different plant and animal sources. Depending on their size and extraction process, cellulose nanocrystals may be referred to as cellulose nanowhiskers (CNW) or nano-crystalline Cellulose (NCC) [12, 13], and cellulose nanofibrils may be referred to as nano-fibrillated cellulose (NFC) or micro-fibrillated cellulose (MFC) [14].

The cellulose content in Ragi Stalk (RS) is 35%, and the average length of the Ragi stalk is 0.5 m, as compared with other sources to prepare nanocellulose. Due to its lower lignin content (5-6%) and shorter growing cycle (approximately 80 days), it is widely suggested as a superior starting material for nanocellulose

production [15, 16]. For the extraction of cellulose and NC, numerous plants, such as the husk of coconut rice and maize, flax, sugar cane bagasse, etc., have been researched [17]. Because of its high strength and stiffness, it is recommended for the production of NC. Hence, Ragi stalk is therefore strongly found well suitable for the nano-cellulose synthesis, due to its availability in abundance and its feasibility. The low lignin content in the Ragi stalk also made it more appropriate for nanocellulose synthesis. Two common processes have been developed for nanocellulose synthesis: the chemical method involving acid hydrolysis of nanocellulose, and the oxidation method, which uses TEMPO (2,2,6,6-tetramethylpiperidine-1-oxyl). Due to its diverse features, availability, and flexibility in reuse, the green synthesis by using the ionic liquid (IL) approach has been replacing these conventional methods in recent years. Naturally occurring cellulose is insoluble in most of the solvents. However, it is soluble in IL.

Ionic liquids are a type of salt composed of cations and anions that are liquid at the ambient temperature and are referred to as green solvents. The increased use of these compounds in the pre-treatment of lignocellulosic biomass is due to their unique physicochemical characteristics including adequate thermal and chemical stability, a low vapour pressure, and a high biopolymer-solvating capacity. The common ionic liquids for dissolving cellulose include 1-butyl-3-methylimidazolium chloride (BmimCl), 1-allyl-3-methylimidazolium chloride (AmimCl), and 1-ethyl-3-methylimidazole acetate [18]. The recent research has identified ionic liquids as suitable solvents, swelling agents, and catalysts for nanocellulose synthesis. The major benefit of employing IL as a pre-treatment is the reproducibility of insolvency recovery with the minimum loss. It has been established that

more than ninety percent of BmimCl's activity can be recovered by reusing it four times without losing its potency [19]. The IL use as a nanocellulose surface modification medium has applications in nanomedicine and drug delivery, according to other researchers [20]. IL has recently been recommended as a reaction media for the homogenous production of cellulose. Therefore, according to some researchers, the homogeneous cellulose acetylation can be accomplished in AmimCl without the need for catalysts, resulting in cellulose acetates with a wide range of

substitution degrees [21]. The purpose of this research is to synthesize nanocellulose from Ragi stalk, as displayed in Figure 1. FT-IR, X-Ray Diffraction, Scanning Electron Microscope, TEM, and Thermo Gravimetry studies were used to examine the effects of ionic liquid treatment on dissolution, morphology, thermal stability, crystallinity, and size in all three cellulosic materials. IL does not contribute to acid waste and is a more environmentally friendly method of isolating nanocellulose compared with conventional studies [22].

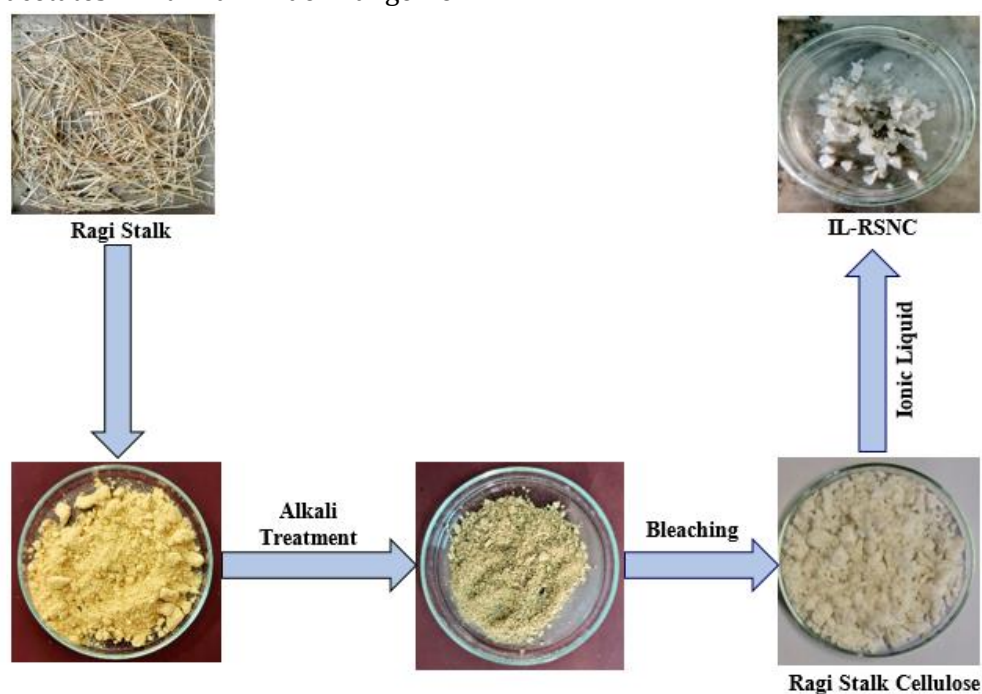


**Figure 1.** Scheme of green synthesis of nanocellulose

## Experimental

### Materials and methods

The Lignocellulosic material such as Ragi Stalk was collected from farmLands in and around Davanagere, Karnataka, India. The chemicals such as Chlorobutane ( $C_4H_9C$ ) and 1-methylimidazole ( $CH_3C_3H_3N_2$ ) were bought from Sigma Aldrich.  $NaClO_2$ ,  $NaOH$ , and  $CH_3COOH$  were purchased from Merck and

Qualigens Chemicals. All chemicals have a purity of 98 to 99% and are used as such without purification.

### Alkali treatment

10 g of finely ground, sieved Ragi stalk Powder treated with a 5%  $NaOH$  solution for 2 hours at temperatures ranging from 85 to 100 °C to remove Wax, Pectin, and hemicellulose. The obtained mass was filtered by repeated

rinsing with distilled water until it reached a pH of 7. After that, the product is oven-dried for a day or until it reaches a constant weight. This process makes fibres more susceptible to bleaching, and further chemical modification.

#### *Bleaching treatment-Pulping*

After being treated with alkali, the sample was bleached to remove any remaining lignin. Alkali-treated samples were treated with a 5% sodium chlorite solution. Then, the mixture was refluxed by using a thermomagnetic stirrer between 90 and 100 °C for 3-4 hours by drop-wise addition of acetic acid to maintain acidic pH. The repetitive washing was done with distilled water eliminates residual lignin. The synthesized cellulose was filtered by deionized water washing until it reached a neutral pH. The obtained mass was oven-dried for one day or till it yields the constant weight and stored for further process.

#### *Synthesis of Ionic Liquid (1-butyl-3-methylimidazolium chloride)*

The two-necked round-bottomed flask containing 60 mL of 1-methyl imidazole (0.61 mol) and 80 mL of Chlorobutane (0.76 mol) was immersed in an oil bath to ascertain constant temperature. The mixture was kept for overnight refluxing at about 115-120 °C in an oil bath with a magnetic stirrer until it gives yellow coloured transparent phase. After cooling the reaction mixture with ice cold water, the pure product was obtained in the form of an oil or solid.

#### *Nanocellulose synthesis in 1-butyl-3-methylimidazolium chloride ionic liquid solvent*

It is synthesized by adding 10 g of 1-butyl-3-methylimidazolium chloride ionic liquid into a 100 mL dry two-necked flask fitted with a water-cooled condenser and carries calcium

guard tube at the outlet of the condenser to avoid moisture entry. Then, it was placed in an oil bath to ascertain constant temperature. 1 g of finely ground and dried Ragi Stalk Cellulose (RSC) was added slowly into a flask containing above ionic liquid and refluxed on a thermomagnetic stirrer at 120-125 °C for 1.5 hours. By dissolving cellulose in ionic liquid, a pale-yellow solution was obtained. After that, the mixture was conciliated by adding 50 mL of ice-cold distilled water. The resulting nanocellulose precipitate was filtered, washed 5-6 times with cold distillate water, dried, stored, and used as IL-RSNC.

#### *Cellulose dissolution in ionic liquid*

Graenacher [23] has filed a patent on the use of molten quaternary ammonium salts in the cellulose production, in which ionic liquids have been used to directly synthesize cellulose solutions. Swatloski *et al.* [24, 25] hypothesized that ionic liquid (combinations of halide anions and imidazolium cations) can dissolve cellulose directly with only the modest heating/microwaving. Furthermore, some research groups have demonstrated that a mixture of ionic liquid combinations and conditions can dissolve cellulose [26]. The anion of the ionic liquid interacts favourably via hydrogen bonding with the hydroxyl protons of cellulose, thereby breaking the strong intermolecular hydrogen bonds that exist between carbohydrate chains and promoting dissolution [27].

#### *Characterizations*

The synthesized nanocellulose sample was analyzed by the instrumentation techniques mentioned here. The FTIR was recorded with Thermo Nicolet iS50. After being mixed with KBr powder, the sample was pressed into thin pellets. The sample's wavelength range was

measured to be between 4000 and 400  $\text{cm}^{-1}$ . The XRD data was recorded by using a Bruker D8 Advance Diffractometer. The crystalline and amorphous zone peak heights were measured, and the crystallinity index (CI) was calculated by using Scherer's formula with a 0.02 step size. The Jeol 6390LA/ OXFORD XMX N instrument used to capture SEM (Scanning Electron Microscopy) images had an acceleration voltage range of 0.5 to 30 kV. A secondary electron (SE) detector was used to acquire the images. TEM images were recorded by using a 200 kV, LaB6 electron gun with a 0.23 nm point resolution, and 0.14 nm lattice resolution. TGA (Thermogravimetric Analysis) and DTA were performed by using the Perkin Elmer STA 6000 instrument (Differential Thermal Analysis).

## Results and Discussion

### FT-IR analysis

The chemical functional groups of cellulose were investigated by using FT-IR. FT-IR of Cellulose and IL-RSNC is depicted in Figure 2, that both have similar cellulose-I structured

absorption peaks between 3321.59 and 3331.89  $\text{cm}^{-1}$ , owing to -OH stretching vibrations caused by hydrogen bonding. The peaks at 2893.39 to 2901.02  $\text{cm}^{-1}$  denotes the C-H stretching vibrations. Whereas, the peaks between 1636.23 and 1641.31  $\text{cm}^{-1}$  are caused by the H-O-H deformation of absorbed water and conjugated C=O stretch vibrations. The region of absorption between 1428.27 and 1157.25  $\text{cm}^{-1}$  was attributed to the asymmetric C-H deformation, which shifted to a low wavenumber and became weaker due to a reaction at higher temperatures with IL. The breaking of H-bonding was at O-6. The C-O anti-symmetric bridge stretching is represented by the peak in the range 1157.25 to 1161.34  $\text{cm}^{-1}$ . The C-O-C pyranose ring skeletal vibration was assigned peaks ranging from 1029.99 to 1045.96  $\text{cm}^{-1}$ . In cellulose, the peaks at 897.09  $\text{cm}^{-1}$  correlate to glycosidic linkage whereas it disappeared in IL-RSNC. Absorption peaks moving to the higher wavenumbers showed the transition from cellulose I to cellulose II. The result revealed that there was no intervening reaction in the middle of the dissolving process.

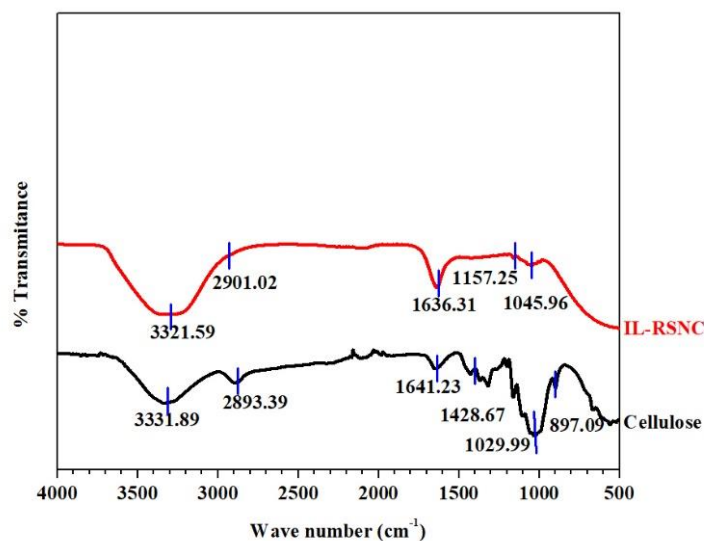


Figure 2. FT-IR of cellulose and IL-RSNC

### XRD analysis

The XRD analysis shows that nanocellulose can be found to be crystalline. Figure 3 displays the X-ray diffraction patterns of IL-RSNC treated with ionic liquid. These XRD patterns depict typical patterns of semi-crystalline materials with an amorphous wide hump and crystalline peaks. IL-RSNC exhibits its  $2\theta$  values in the range between  $15.50^\circ$ ,  $22.474^\circ$ , and cellulose shows the peaks at  $15.50^\circ$  and  $22.50^\circ$ . Due to the disruption of intermolecular and intramolecular hydrogen bonds of cellulose by the ionic liquid, the crystallinity index of the synthesized nanocellulose is reported to be slightly decreased than that of origin cellulose.

### SEM analysis

The high-resolution surface imaging is possible by using a scanning electron microscope. By using an electron beam, the SEM produces images of the surface. The prepared nanocellulose was found to be fibrous with considerable aggregation, as seen by SEM images (Figure 4). The surface morphology and average size are depicted in the SEM images. This shows nanoscale dimensions, including the uneven cross-sections, a vast number of

microscopic microfibrils, various forms, and non-uniform surfaces. The IL-RSNC morphology corresponds to nano-sized fibres in the form of regular structured bundles. Here, individualized nanofibers can be obtained with the ultrasonic treatment.

### TEM analysis

The TEM images of IL-RSNC were obtained to analyse the internal morphology and structure of the synthesized nano cellulose, as displayed in Figure 5. The TEM image indicates that the obtained nanocellulose is in the form of nanofibers. Nanofibers are distinct in the form of bundles and readily visible. Even the tendency to agglomerate can be seen. The IL-RSNC reveals nanofiber bundles with an average diameter between 14.58 and 22.17 nm and the length in terms of microns that are regularly organized. This is inferred from the above observation that the synthesized nanocellulose well exhibits nanoscale dimensions. The structured nanofiber bundles can be seen in IL-RSNC. The above analysis reveals that the ionic liquid readily dissolves the cellulose affecting the structure, morphology, and size distribution of the synthesized nanocellulose.

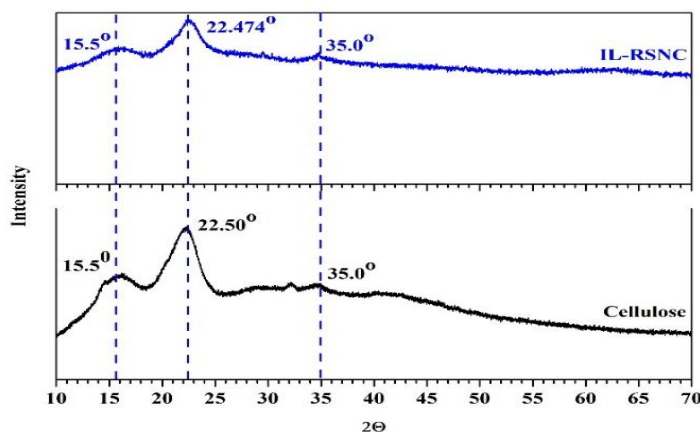


Figure 3. The XRD pattern of IL-RSNC and cellulose

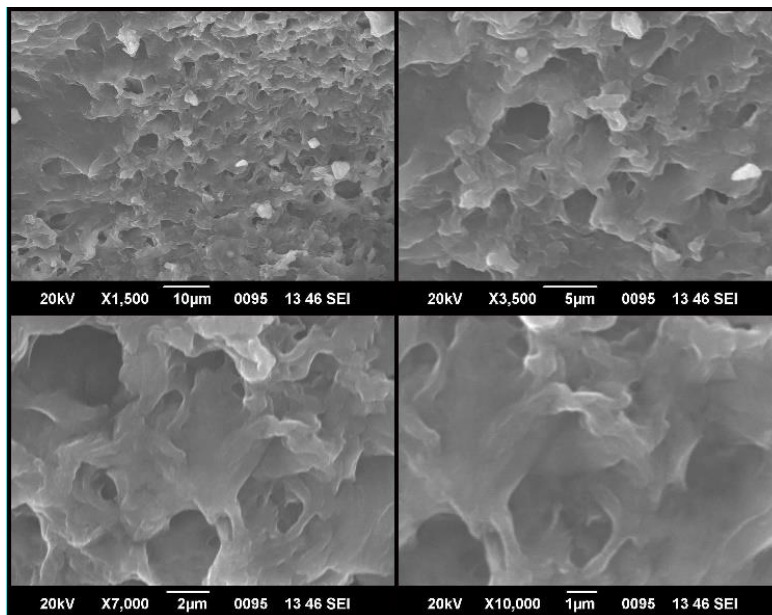


Figure 4. SEM monographs of IL-RSNC

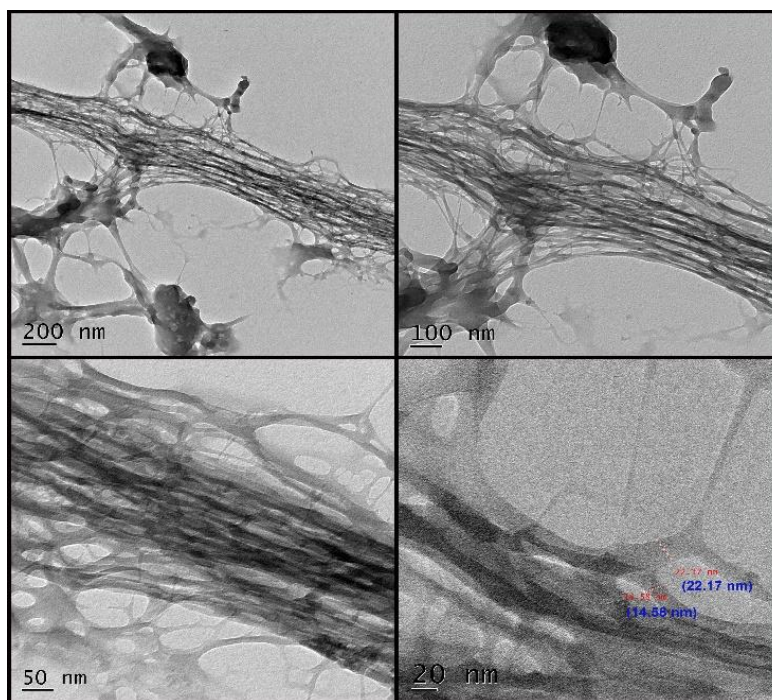


Figure 5. TEM Image IL-RSNC

*TGA/DTA analysis*

The thermal stability of the IL-RSNC was examined by using TGA, and the DTA curves are shown in Figures 6 and 7, respectively. Here, the

weight loss occurred in three stages in the first stage, the water evaporation in the synthesized nanocellulose is observed between 80 °C to 110.0 °C. The second and the third stage degradation depicts the major weight loss



between 250.0 °C to 329.5 °C regions indicating the hemicellulose depolymerization, glycosidic linkages, and they have broken. The onset degradation temperature is found to be 240 °C.

Here, the weight loss occurred in three stages. The results depict that the significance of IL-treated is that the synthesized nanocellulose indicates superior thermal stability of 459.9 °C.

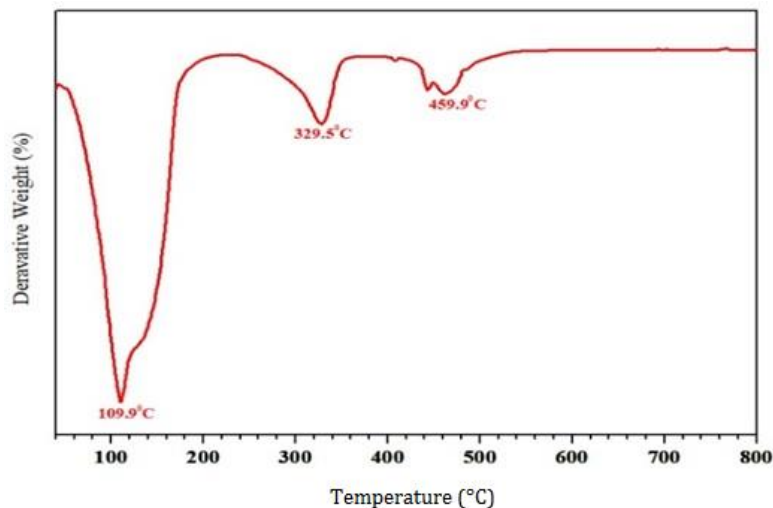


**Figure 6.** TGA of IL-RSNC

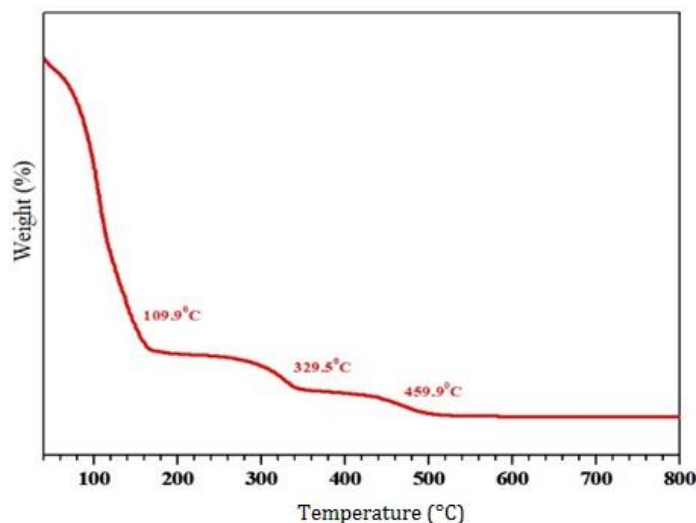


**Figure 7.** DTG of IL-RSNC

## Conclusion

In the present study, RS is an abundantly available lignocellulosic agricultural biomass utilized to produce nanocellulose from an ionic liquid. The FTIR spectra suggest that IL-RSNC exhibits the same distinctive cellulose peaks.

The finding reveals that there was no derivational reaction during the cellulose dissolution process. According to the X-ray crystallographic investigations, produced nanocellulose consists of semi-crystalline materials with an amorphous wide hump and crystalline peaks. It implies that the hydrogen

bonds of cellulose were disrupted, resulting in the disintegration of the crystal structure during the entire process. Different shapes with a non-uniform surface, regular cross-sections, and a great number of microscopic microfibrils can be seen in the SEM images. The TEM images show that the synthesized cellulose is in the nano-scale dimension. Cellulose is apparently dissolved by the ionic liquid, a promising green solvent, which impacts the morphology and size distribution of the produced Ragi stalk in the nanometre size. According to TGA/DTA analysis, samples exhibit a minor weight loss of roughly 80-100 °C, which is attributed to the evaporation of water bound in the cellulose samples. The strong troughs in the DTA curve reveal that the breakdown onset of ionic liquid treated cellulose is 240 °C. TGA revealed that IL-RSNC treated with ionic liquid has a higher degradation temperature (459.9 °C), indicating a greater thermal stability. Therefore, this research shows a new perspective to synthesize the high-strength nanocomposites and the high-temperature resistant materials for the removal of heavy metals and demonstrates the remarkable practical application of nanocellulose from agricultural biomass by a greener pathway, which will undoubtedly address India's need for the solid waste management and reduce chemical waste through a more realistic approach.

### Disclosure Statement

No potential conflict of interest was reported by the authors.

### Funding

This research did not receive any specific grant from funding agencies in the public, commercial, or not-for-profit sectors.

### Authors' contributions

All authors contributed to data analysis, drafting, and revising of the paper and agreed to be responsible for all the aspects of this work.

### Orcid

Prasanna Kumar Jammapura Kallappa   
0000-0002-9249-5359

### References

- [1]. Sharma A., Mohanty B. *RSC Advances*, 2021, **11**:13396. [[Crossref](#)], [[Google Scholar](#)], [[Publisher](#)]
- [2]. Katare V.D., Madurwar M.V. *Construction and Building Materials*, 2017, **152**:1 [[Crossref](#)], [[Google Scholar](#)], [[Publisher](#)]
- [3]. Youshizawa S., Tanaka M., Shekder A.V. *Global Trends in Waste Generation In Recycling, Waste Treatment, and Clean Technology*, TMS Mineral, Metals and Materials Publishers, Spain, 2004, 1541 [[Publisher](#)]
- [4]. Jagadesh P., Ramachandramurthy A., Murugesan R. *Construction and Building Materials*, 2018, **176**:608 [[Crossref](#)], [[Google Scholar](#)], [[Publisher](#)]
- [5]. Reddy N., Yang, Y. *Green Chemistry*, 2005, **7**:190 [[Crossref](#)], [[Google Scholar](#)], [[Publisher](#)]
- [6]. Lin N., Dufresne A. *European Polymer Journal*, 2014, **59**:302 [[Crossref](#)], [[Google Scholar](#)], [[Publisher](#)]
- [7]. Das S., Ghosh B., Sarkar K. *Sensors International*, 2022, **3**:100135. [[Crossref](#)], [[Google Scholar](#)], [[Publisher](#)]
- [8]. Klemm D., Kramer F., Moritz S., Lindström T., Ankerfors M., Gray D., Dorris A. *Angewandte Chemie International Edition*, 2011, **50**:5438. [[Crossref](#)], [[Google Scholar](#)], [[Publisher](#)]
- [9]. Baker S., Satish S. *Int. J. Bio-Inorg. Hybd. Nanomat*, 2012, **1**:67 [[Publisher](#)]
- [10]. Kavitha K.S., Baker S., Rakshith D., Kavitha H.U., Yashwantha Rao H.C., Harini, B.P. and Satish S. *Int Res J Biol Sci*, 2013, **2**:66 [[Publisher](#)]

- [11]. Wegner T.H., Jones P.E. *Cellulose*, 2006, **13**:115 [[Crossref](#)], [[Publisher](#)]
- [12]. Fortunati E., Puglia D., Monti M., Peponi L., Santulli C., Kenny J.M., Torre L. *Journal of Polymers and the Environment*, 2013, **21**:319 [[Crossref](#)]
- [13]. Dong H., Snyder J.F., Tran D.T., Leadore J.L. *Carbohydrate polymers*, 2013, **95**:760 [[Crossref](#)], [[Google Scholar](#)], [[Publisher](#)]
- [14]. Bledzki A.K., Gassan J. *Progress in polymer science*, 1999, **24**:221 [[Crossref](#)], [[Google Scholar](#)], [[Publisher](#)]
- [15]. Matano C., Meiswinkel T.M. *Wendisch Wheat and rice in disease prevention and health*, Academic Press, 2014, 493 [[Crossref](#)], [[Google Scholar](#)], [[Publisher](#)]
- [16]. Lamichhane G., Khadka S., Acharya A., Parajuli N. *Biomass Conversion and Biorefinery*, 2021, **1** [[Crossref](#)], [[Google Scholar](#)], [[Publisher](#)]
- [17]. Hussain M., Tufail T., Saeed F., Ain H.B.U., Shahzadi M., Suleria H.A.R. *Bioactive Compounds from Multifarious Natural Foods for Human Health*, 2022, 43 [[Publisher](#)]
- [18]. Babicka M., Woźniak M., Szentner K., Bartkowiak M., Peplińska B., Dwiecki K., Borysiak S., Ratajczak I. *Materials*, 2021, **14**:3264 [[Crossref](#)], [[Google Scholar](#)], [[Publisher](#)]
- [19]. Phanthong P., Karnjanakom S., Reubroycharoen P., Hao, X., Abudula A., Guan G. *Cellulose*, 2017, **24**:2083 [[Crossref](#)], [[Google Scholar](#)], [[Publisher](#)]
- [20]. Haron G.A.S., Mahmood H., Noh M.H., Alam M.Z. and Moniruzzaman M. *ACS Sustainable Chemistry & Engineering*, 2021, **9**:1008. [[Crossref](#)], [[Google Scholar](#)], [[Publisher](#)]
- [21]. Turner M.B., Spear S.K., Holbrey J.D., Rogers R.D. *Biomacromolecules*, 2004, **5**:1379 [[Crossref](#)], [[Google Scholar](#)], [[Publisher](#)]
- [22]. Pal N., Hoteit H., Mandal A. *Journal of Molecular Liquids*, 2021, **339**:116811 [[Crossref](#)], [[Google Scholar](#)], [[Publisher](#)]
- [23]. Graenacher C.U.S. Patent, 1931 1,943,176. [[Crossref](#)]
- [24]. Swatloski R P., Spear S K., Holbrey J D. and Rogers R.D. *J. Am. Chem. Soc*, 2002, **124**:4974 [[Crossref](#)], [[Google Scholar](#)], [[Publisher](#)]
- [25]. Swatloski R P., Holbrey J.D., Rogers R.D. 2002, U.S. Patent 6,824,599 B2 [[Crossref](#)], [[Publisher](#)]
- [26]. Wang H., Gurau G., Rogers R.D. *Chem. Soc. Rev*, 2012, **41**:1519 [[Crossref](#)], [[Google Scholar](#)], [[Publisher](#)]
- [27]. Remsing Richard C., Swatloski Richard P., Rogers Robin D., Guillermo M. *Chemical Communications*, 2006, **12**:1271 [[Crossref](#)], [[Google Scholar](#)], [[Publisher](#)]

**How to cite this manuscript:** Prasanna Kumar Jammapura Kallappa\*, Prakash Gowdra Kalleshappa, Suresh Basavarajappa, Basavarajappa Bachi Eshwarappa. Green synthesis of nanocellulose fibers from ragi stalk and its characterization. *Asian Journal of Green Chemistry*, 6(3) 2022, 273-283. DOI: 10.22034/ajgc.2022.3.7